

AERODYNAMIC CHARACTERISTIC COMPARISON OF THE FORWARD AND BACKWARD-SWEPT WINGS

XUE RongRong*, YE ZhengYin*, WANG Gang*

*School of Aeronautics, Northwestern Polytechnical University, Xi'an, 710072, China

Keywords: Aerodynamic characteristic; Forward-swept wing; back-swept wing; Momentum flux

Abstract

Swept angle can increase positively the drag divergence Mach number of wing which results in dramatic improvement of the maximum speed of modern aircraft. Forward swept wings in fact totally are not utilized at all for its potential aeroelastic divergence issues. However, knowledge on the aerodynamic characteristic of forward swept wings is greatly different among researchers. Simplified models are constructed to compare the influence of swept angle on aerodynamic characteristic of the forward and backward swept wings. For both forward- and backward-swept wing models, the wing planform has a leading- and trailing-edge sweep of $-45/45$ degree and was untapered. The wing span of 4 meter, in conjunction with a chord length of 1 meter, yielded an aspect ratio of 4. Here flow phenomenon on the forward-and back swept wings are reproduced by solving Reynolds-averaged Navier-Stokes Equations through Computational Fluid Dynamic (CFD) technique in the paper. The numerical calculation used half models of the wings to reduce the computational load efficiently. Based on the same structural grid CFD computation were conducted by FLUENT CFD software at Mach number 0.2 and Reynolds number $4.6E6$ based on the mean aerodynamic chord length of the wings. Comparisons of the force coefficients between forward- and backward-swept wings show the back-swept wing generates a higher lift coefficient and a higher lift slope than forward-swept wing before the stalling angle,

which means that back swept wing has a higher maximum lift coefficient while in fact a smaller stalling angle than forward swept wings as can be predicted. Meanwhile the recorded data actually shows lift curve of forward-swept wing gradually changed at the stalling angle which reflects its better stall performance than the backward. The drag curves demonstrate that forward-swept wing has a lower drag coefficient than the backward at small angle of attack which benefits from the elliptical lift distribution. However situation changes to totally opposite after AOA 8° mainly caused by the separation at the forward swept wing root which leads to dramatic drop of the z direction momentum flux and the increase of the pressure drag shown in the C_{dp} figure. The integrals of the forces/momentum flux was carried out to explain how the aerodynamic characteristic presents for both wings. Spanwise lift distribution shows that the forward swept wing is very similar to the ideal elliptical distribution which generate better aerodynamic performance. However with the increase of angle of attack, Y direction momentum flux became bigger and bigger which leads to flow obstruction at the forward swept wing root resulting in significantly drop of the wing root Z direction momentum flux, which means less lift and more drag are produced.

1 Introduction

The concept of swept wing was first investigated as early as 1935, which has the effect of delaying the aerodynamic drag rise caused by fluid compressibility near the sound of the speed. The term “swept wing” is normally used to mean “back swept wing” because the back swept wing is the most developed and widely utilized wing. The forward swept wing, which was developed at the same time, was only used at several aircraft, for example, the forward swept wing technology demonstration aircraft X-29A published at 1970s by USA, which is the most famous one. The unpopularity of the forward swept wing is mainly caused by one disadvantage: aeroelastic torsional divergence of the wing^[1].

The problem is caused by aerodynamic center positioned ahead of the wing’s stiffness center, whereas the opposite is true for back swept wing. The aerodynamic forces in fact would strengthen the torsional deformation at the wingtip and the increased torsional deformation further generated more forces. If the structure stiffness is not big enough to resist the force, the structural damage seems to be unavoidable. This phenomenon is called aeroelastic torsional divergence^[2]. In fact the general method to solve this problem is to increase the stiffness of the wing structure, however the penalty of the structure weight is unacceptable. Fortunately the problem had been solved by adopting aeroelastic tailoring technology of composite material on X-29A.

Von B.R.A Bums summarized the advantages of the forward swept wing by comparing with backward swept wing with same wing span and taper ratio based on Prandtl lifting line theory as follows: (1) smaller reduced drag; (2) bigger lift slope; (3) gradually decreased head up tendency; (4) smaller structure wing span; (5) smaller mass compared to the equivalent backward swept wing; (6) flow separation first starts at the root of forward swept wings which can effectively improve the aileron effectiveness and roll damp. MJ Mann demonstrated that with the advent of advanced composite materials, supercritical airfoils, fly-by-wire, and canard technology, forward swept wing provides the potential for increased aerodynamic efficiency, improved

low speed handling, reduced approach speed, and departure resistance^[3].

During the design of the forward swept wing technology demonstration aircraft X-29A, NASA conducted wind tunnel tests on the wing body adopting symmetric elliptical airfoil. The longitudinal aerodynamic performance of forward swept wing with leading edge swept angle 32° and backward swept wing with leading edge angle 60° was obtained at Mach number 0.3, Reynolds number 1.4 million. Results shows that lift slope of forward swept wing is smaller than backward wing, and the maximum lift coefficient of forward swept wing ($c_{l_{max}} = 0.96$, $\alpha_{c_{l_{max}}} = 40^\circ$) was also smaller than backward wing^{[4][5]}. However forward swept wing’s stalling performance was far better. In fact at low speed wind tunnel test the aerodynamic performance seemed to be not such better as described by Prandtl lifting line theory^[6].

In Embry-Riddle Aeronautical University Lance W. Traub^[7] also brought low speed wing tunnel test on strip location’s effects on both forward- and backward- arrow wing’s longitudinal performance. The test was carried out at wind speed 25m/s and $Re=180000$ on two untapered wings with swept angle of -65° and 65° , aspect ratio of 2. The experiment data illustrates forward arrow wing’s lift is small than backward wing when angle of attack (AOA) is smaller than 4° , the leading edge strip shift the forward wing’s lift obviously better than backward wing. Wing’s surface pathlines indicates forward swept wing separates at the wing root which is on the contrary for backward wing.

Forward swept wings shows a great performance during the NASA X-29A flight tests that was confirmed by Russia’s Su-47 forward swept demonstration aircraft from the released news. However the flow mechanic of forward swept was seldom researched and general understanding on its aerodynamic characteristics is not formed, many misunderstandings still troubles the researchers. The paper takes advantage of CFD technique to

simulate the flow field of simplified wing models to obtain the low speed aerodynamic performance of forward- and backward- swept wings and analyze the difference of their flow mechanics.

2 CFD Computation & Procedure

CFD computation were conducted by FLUENT CFD software at Mach number 0.2 and Reynolds number 4.6 million based on the mean aerodynamic chord length of the wings and post-processed by Tecplot. For both forward- and backward-swept wing models, the wing planform has a leading- and trailing-edge sweep of 45/-45 degree which were both not tapered. The wing span of 4 m, in conjunction with a chord of 1 m, yielded an aspect ratio of 4. The numerical calculation used half model of the wings to reduce the computational load efficiently. The far field boundary was set at 100 times of the mean aerodynamic chord length away from the wing surface. Meanwhile structural grid was adopted to discrete the whole flow field with surface grid $y+=1$. The number of surface grid of wings was 12176, and the total number of the volume mesh was 6802039. The surface grid, boundary layer grid and the far field are shown in Figure 1-3.

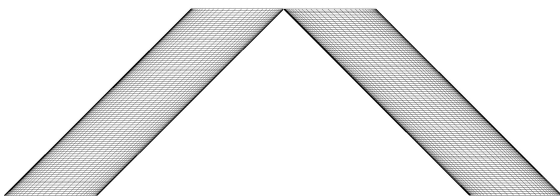


Figure 1 Surface grid of forward- and backward-swept wing

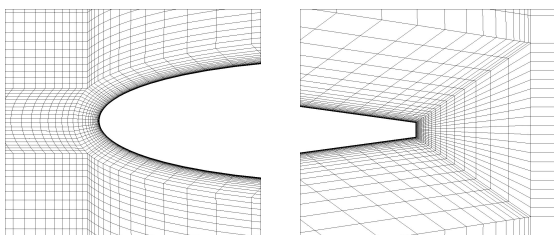


Figure 2 Boundary layer grid

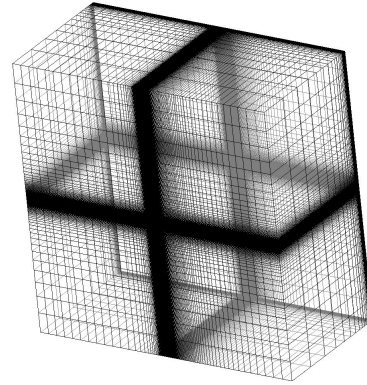
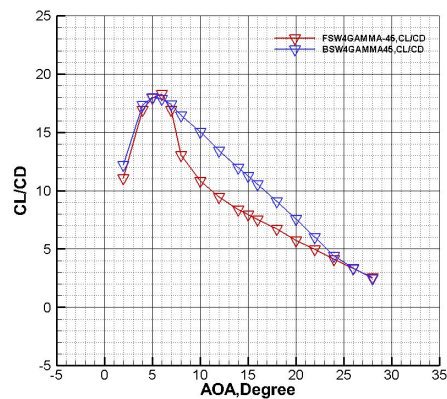
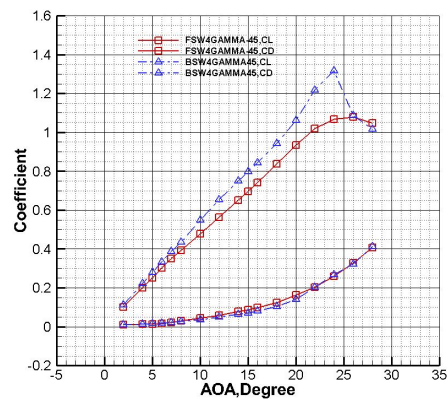


Figure 3 Far field boundary grid

3 Results & Discussion

CFD data is obtained at AOA $2^\circ \sim 28^\circ$ which shows comparisons of the force coefficients of both forward- and backward-swept wings in Figure 4.



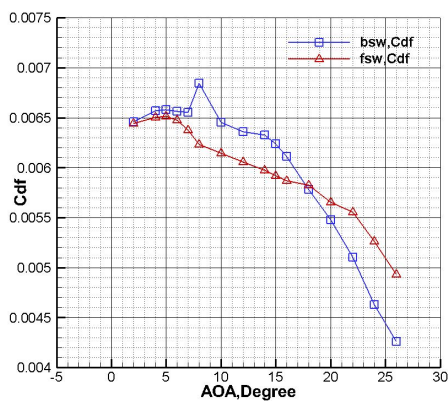
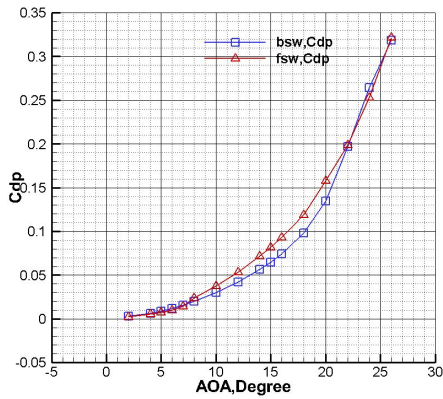


Figure 4 Lift , drag , lift/drag, viscous drag and pressure drag curves of forward- and back-swept wing

As can be seen in Figure 4, the forward-swept wing shows a lower lift coefficient and a lower lift slope than backward-swept wing for AOA (angle of attack) < 26 degree while a higher one for AOA > 26°. The backward-swept wing has a significantly higher maximum lift coefficient 1.3180 at AOA 24 ° than forward-swept wing which has the maximum lift coefficient 1.0773 at AOA 26°.

As can be predicted, the recorded data actually shows lift curve of forward-swept wing gradually changed at the stalling AOA which means its better stall performance than the backward one. The drag curves demonstrate that forward-swept wing has a lower drag coefficient than the backward one when AOA is less than 8°. However at AOA 8° FSW’s drag coefficient increases so much that it becomes bigger than ASW, which is mainly caused by the increase of the pressure drag shown in the 4th figure. Until

the AOA reaches close to stalling AOA, the two wings’ drag come to the same level again which is also caused by the pressure drag increase but of the ASW.

Splitting wing drag into two components: pressure drag and friction drag, it shows that the pressure drag of the wings occupies the majority of the total wing drag. Meanwhile it can be found that the wing friction drag decreases and pressure drag increases with the increase of the AOA, which is mainly caused by the transition of the laminar flow to turbulence flow around the wings. The FSW’s pressure drag is higher than the ASW between the interval of AOA 8° and AOA 24°.

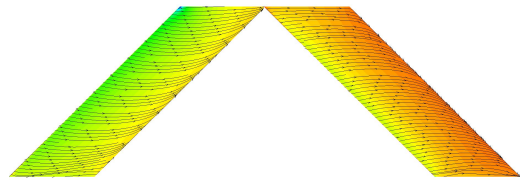


Figure 6 Pathlines on the upper surface of forward-swept wing (L) and back-swept wing (R) at AOA=5°

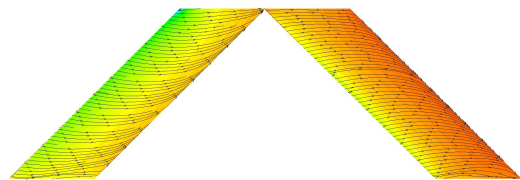


Figure 7 Pathlines on the upper surface of forward-swept wing (L) and back-swept wing (R) at AOA=6°

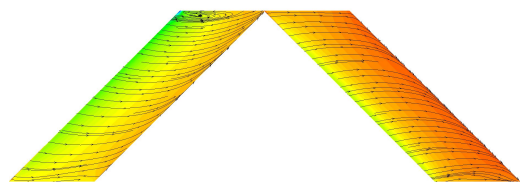


Figure 8 Pathlines on the upper surface of forward-swept wing (L) and back-swept wing (R) at AOA=7°

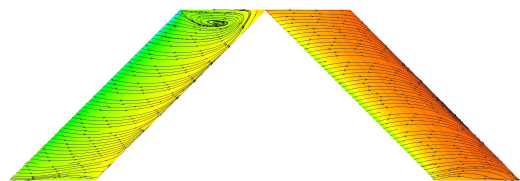


Figure 9 Pathlines on the upper surface of forward-swept wing (L) and back-swept wing (R) at AOA=8°

AERODYNAMIC CHARACTERISTIC COMPARISON OF THE FORWARD AND BACKWARD-SWEPT WINGS

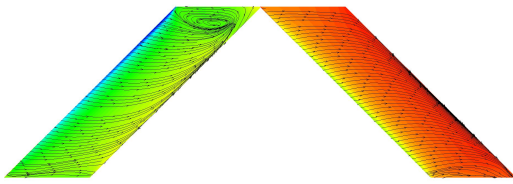


Figure 10 Pathlines on the upper surface of forward-swept wing (L) and back-swept wing (R) at AOA=10°

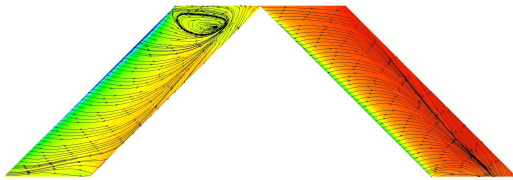


Figure 11 Pathlines on the upper surface of forward-swept wing (L) and back-swept wing (R) at AOA=15°

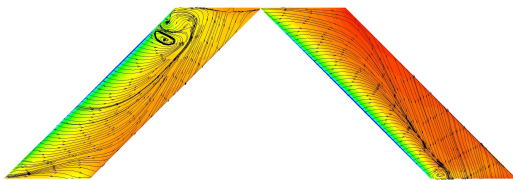


Figure 12 Pathlines on the upper surface of forward-swept wing (L) and back-swept wing (R) at AOA=20°

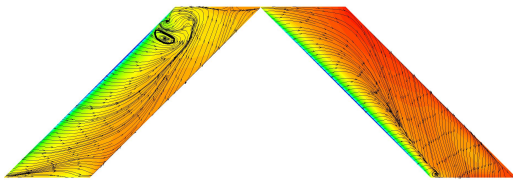


Figure 13 Pathlines on the upper surface of forward-swept wing (L) and back-swept wing (R) at AOA=22°

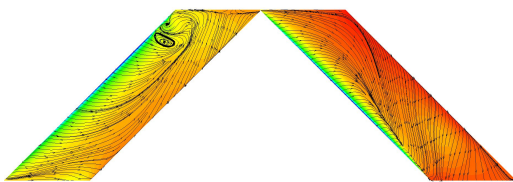


Figure 14 Pathlines on the upper surface of forward-swept wing (L) and back-swept wing (R) at AOA=24°

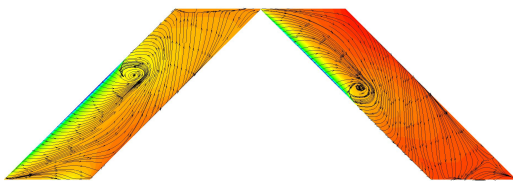


Figure 15 Pathlines on the upper surface of forward-swept wing (L) and back-swept wing (R) at AOA=26°

Figure 8 shows at AOA of 7° a small reverse flow region appears at the root of the FSW, then develops suddenly to almost 15% wing area when AOA increases to 8°. With the increase of the AOA, this reverse flow region keeps expanding and the position of the vertex core is pushed to the leading edge, while the spanwise flow was strengthened. The main character of FSW is to maintain excellent performance at the outer wing to obtain a better control efficiency and stalling performance because the stalling mainly happened at the wing root and at the wing tip enough lift force was still obtained even if the AOA is reaching the stalling AOA (in this case which is 26°). However the BSW basically generated no reverse flow at the whole wing area until AOA 15° when reverse flow firstly appeared at the wing tip and developed to wing root direction. At AOA 24° almost 70% wing area was completely stalling which instantly leads to a drop of the lift coefficient.

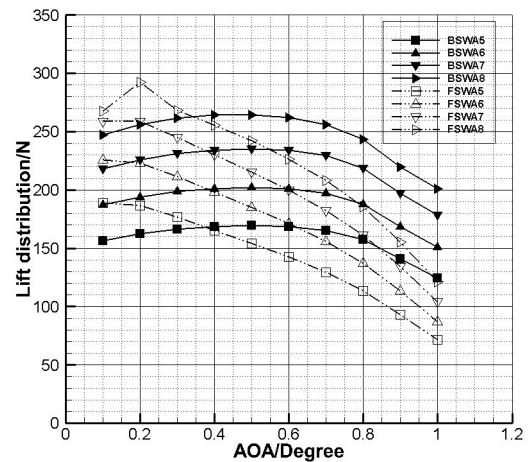


Figure 16 Lift distribution along the forward- and back-swept wing at different AOA

By extracting lift at different spanwise position shown in figure 16, The FSW's spanwise lift distribution is more similar to the ideal elliptical distribution than the ASW wing, which is bigger at the inner FSW and smaller at the outer FSW than ASW. Theoretically speaking the distribution should bring the FSW a better

aerodynamic performance, however the lift at the outer FSW reduces so fast that in fact negative influence appears to the total lift of the wing. Considering that no installation angle is taken into account in the wing's design, the addition of the installation angle may lead to a positive effect. This phenomenon is directly influenced by the z direction momentum flux flowing by the wing surface. Momentum flux at z direction is shown in figure 17, which demonstrates the same tendency of C_l spanwise distribution. At AOA 8° momentum flux drops heavily at FSW wing root that is also the separation expanding shown in the figure 9. This flow separation is mainly caused by the spanwise flow. In figure 19, FSW and ASW have opposite y direction momentum flux, which means FSW flows toward wing root while ASW flows toward wing tip. Accumulation of boundary layer brought by y momentum straightly leads to the separation and lift reduce at the FSW root.

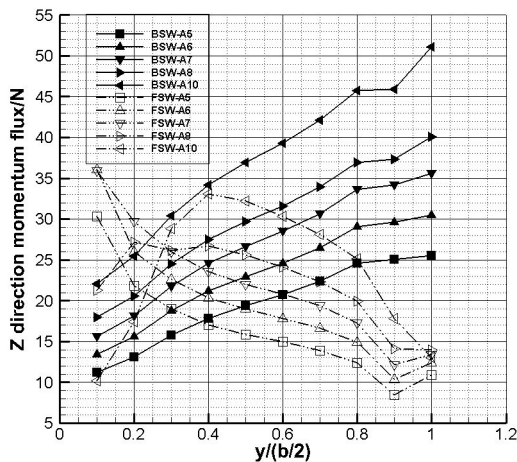


Figure 17 Z direction momentum flux distribution along the forward - and back -swept wing at different AOA

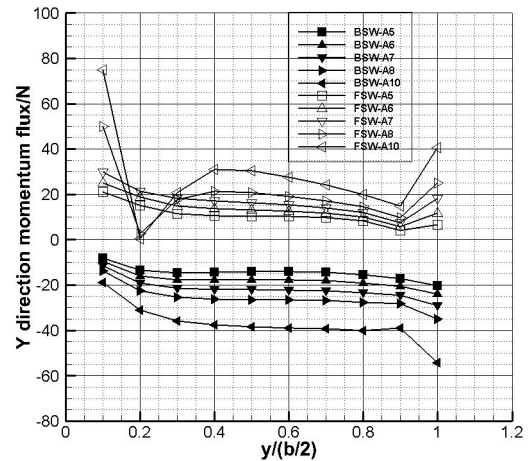


Figure 18 Y direction momentum flux distribution along the forward - and back -swept wing at different AOA

4 Conclusion

The flow field of forward-and back swept wings are reproduced by solving Reynolds-averaged Navier-Stokes Equations through FLUENT CFD in the paper at Mach number 0.2 and Reynolds number 4.6 million. The results illustrate:

1. Comparisons of the force coefficients between forward- and backward-swept wings show the back-swept wing generates a higher lift coefficient and a higher lift slope than forward-swept wing before the stalling angle, which means that back swept wing has a higher maximum lift coefficient.
2. The recorded data actually shows lift curve of forward-swept wing gradually changed at the stalling angle and a bigger stall AOA which reflects its better stall performance than the backward.
3. The drag curves demonstrate that forward-swept wing has a lower drag coefficient than the backward at small angle of attack which benefits from the elliptical lift distribution. However situation changes to totally opposite after AOA 8° mainly caused by the separation at the forward swept wing root which leads to dramatic drop of the z direction momentum flux

and the increase of the pressure drag shown in the Cdp figure.

4. Spanwise lift distribution shows that the forward swept wing is very similar to the ideal elliptical distribution which generate better aerodynamic performance. However with the increase of angle of attack, Y direction momentum flux became bigger and bigger which leads to flow obstruction at the forward swept wing root resulting in significantly drop of the wing root Z direction momentum flux, which means less lift and more drag are produced.

References

- [1] Krone N.J.. Divergence Elimination with Advanced Composite. *AIAA Paper 75-1009*,1975.
- [2] Huffman Jarrett K., Fox Charles H.. Subsonic Longitudinal and Lateral-directional Static Aerodynamic Characteristics for Closed-coupled Wing-Canard Model in Both Swept Back and Swept Forward Configurations. *NASA-TM-74092*,1978.
- [3] Mann M.J., Mercer C.E.. A Forward Swept Wing Fighter Configuration Designed by A Transonic Computational Method. *Journal of Aircraft*, 1986, 23(6):506-512.
- [4] Blair M., Weisshaar T.A.. Wind tunnel experiments on the divergence of swept wings with composite structures. *Aircraft Systems and Technology Conference, Aircraft Design and Technology Meeting. AIAA-81-1670*, 1981.
- [5] Moore M., Frei D.. X-29 Forward Swept Wing Aerodynamic Overview. *Applied Aerodynamics Conference, Fluid Dynamics and Co-located Conferences*, 83-1834, 1983.
- [6] Truckernbrodt E.. How to Improve the performance of transport aircraft by variation of wing aspect-ratio and twist. *12th Congress of the International Council of the Aeronautical Science. ICAS Proceedings*, pp 1-17, 1980.
- [7] Traub Lance W., Lawrence Jesse. Aerodynamic Characteristics of Forward and Aft- Swept Arrow Wings. *Journal of Aircraft*, 2009, 46(4):1454-1457.
- [8] Zhang B, and Laschka B. On Forward Swept-Wing's Aerodynamic Characteristics. *Journal of Northwestern Polytechnical Univ*, 1989, 7(3):321-328.
- [9] Gupta S. C.. Aerodynamic Characteristics of Forward Sweep. *Flight Simulation Technologies Conference and Exhibit, Guidance, Navigation, and Control and Co-located Conferences*.1990-3401,1990.
- [10] Spacht G.. The Forward Swept Wing: A Unique Design Challenge. *AIAA Aircraft Systems Meeting, Anaheim, California*.1980-1885,1980.
- [11] Breitsamter Christian, Laschka Boris. Vortical Flowfield Structure at Forward Swept-Wings Configurations. *Journal of Aircraft*.2001, 38(2):193-207.
- [12] Gerhardt Heiz A, Seho Kenneth, Nolan Joan , Mrdeza Matthew N.. Aircraft with Variable Forward-sweep Wing. *US Patents:5984231*.Nov,6,1998.
- [13] Krone N.J.. Forward Swept Wing Flight Demonstrator. *AIAA Aircraft Systems and technology Meeting, Anaheim, California*.1980-1882,1980.
- [14] Nangia R.K., Palmer M.E.. Flying Wings (Blended Wing Bodies) with Aft- & Forward- Sweep, Relating Design Camber & Twist to Longitudinal Control. *AIAA ATMOSPHERIC FLIGHT MECHANICS Conference & Exhibit, Monterey, California*. 2002-4616, 2002.
- [15] Wright Jan.R, Cooper Jonathan E.. *Introduction to Aircraft Aeroelasticity and Loads*. Wiley,2007.

Contact Author Email Address

zacktashaw@163.com

Copyright Statement

The authors confirm that they, and/or their company or organization, hold copyright on all of the original material included in this paper. The authors also confirm that they have obtained permission, from the copyright holder of any third party material included in this paper, to publish it as part of their paper. The authors confirm that they give permission, or have obtained permission from the copyright holder of this paper, for the publication and distribution of this paper as part of the ICAS proceedings or as individual off-prints from the proceedings.